# A Study of the Crystal Structure and Hydrogen Bonding of 3-Trifluoroacetyloxime Substituted 7-Acetamido-2-aryl-5-bromoindoles

**Malose J. Mphahlele**

Department of Chemistry, College of Science, Engineering and Technology, University of South Africa, Private Bag X06, Florida 1710, South Africa; mphahmj@unisa.ac.za; Tel.: +27-11-670-9301

**Abstract:** The 7-acetyl-2-aryl-5-bromo-3-(trifluoroacetyl)indoles **1a-d** were reacted with hydroxylamine hydrochloride (2.2 equiv.) in the presence of pyridine in ethanol under reflux to afford the corresponding diketo oxime derivatives **2a-d**. Beckmann rearrangement of the latter with trifluoroacetic acid under reflux afforded the corresponding 7-acetamido-2-aryl-5-bromo-3-(trifluoroacetyloxime)indoles **3a-d**. The structures of the prepared compounds were characterized using a combination of NMR ($^1$H & $^{13}$C), IR, and mass spectrometric techniques. The molecular structure of the 3-trifluoroacetyloxime substituted 7-acetamido-2-aryl-5-bromoindoles was unambiguously confirmed by the single crystal X-ray diffraction data of **3d**. Structural studies of **3d** in the solid state by X-ray crystallography provided evidence of hydrogen bonding networks and π-stacking of the indole moiety. Compound **3d** was crystallized in the trigonal space group R-3:H with unit cell dimensions a = 25.1614(13), b = 25.1614(13), c = 17.3032(9) Å, $\alpha = \beta = 90°$, $\gamma = 120°$, V = 9486.9(11) Å$^3$, Z = 6. The density functional theory (DFT) structural parameters (bond lengths, bond angles, and torsion angles) of the optimized geometry calculated using the B3LYP/6-311G basis set were found to compare favourably with those of the X-ray crystal structure.

**Keywords:** 7-acetyl-2-aryl-5-bromo-3-(trifluoroacetyl)indoles; oximation; Beckmann rearrangement; hydrogen bonds; XRD; DFT

## 1. Introduction

The chemistry of indole- and isatin-based oximes has been the subject of numerous studies due to their interesting chemical and biological applications [1]. Oximes generally act as dual hydrogen-bond donors via the –O–H moiety and hydrogen-bond acceptors via the –C=N and the –OH moieties. They are capable of forming dimers as well as oxime-oxime catemers via O–H···N=C and O–H···OH hydrogen-bonds in the solid-state [2]. Hydrogen bonding plays an important role in drug–receptor interactions, and drug design in chemical and biological processes as well as molecular recognition and the bioactivity of macromolecules [3]. Hydrogen bond formation causes changes in the distances between atoms and the rearrangement of electron densities on the groups involved in the interaction and therefore chemical reactivity of the reaction centres that are directly involved in the hydrogen bonding [4]. Structure-activity relationship (SAR) studies of the polysubstituted indoles revealed that an acetyl or formyl group on C-3 of the indole framework facilitates the interaction with biological receptors and therefore enhances anticancer activity [5]. We evaluated the 3-trifluoroacetyl-substituted 7-acetyl- and 7-acetamido-2-aryl-5-bromoindoles as well as their corresponding C-3 unsubstituted precursors for antigrowth properties against the A549 and HeLa cell lines and for their ability to inhibit tubulin polymerization [6]. Only the 3-trifluoroacetyl substituted 7-acetamido-2-aryl-3-bromoindoles

were found to exhibit significant cytotoxicity against the two cancer cell lines and also to inhibit tubulin polymerization. Molecular docking (in silico) of the 2-aryl-5-bromo-3-(trifluoroacetyl)indoles into the colchicine-binding domain of $\alpha,\beta$-tubulin interface predicted the presence of a hydrogen bond between the the amide and 3-trifluoroacetyl moieties with some of the protein residues [6]. The propensity of the amide moiety to serve as a dual hydrogen-bond donor and acceptor plays a significant role in the interaction of bioactive compounds with the receptors [4,7]. A thorough knowledge of hydrogen bond interaction, on the other hand, helps in understanding the chemical properties of organic compounds and bio-macromolecules [8]. Recourse to the literature revealed a paper describing the transformation of a series of $\alpha$-trifluoromethylated ketoximes to afford optically active $\alpha$-trifluoromethylated amines, which are important sources of fluorinated pharmaceuticals [9]. We considered the cytotoxicity of the 2-arylindole derivatives [5,6,10] in combination with the literature SAR analyses on indole oximes [1] to transform the strong hydrogen bond accepting trifluoroacetyl group into dual hydrogen-bond donating and accepting $\alpha$-trifluoromethylated ketoxime function based on the 7-acetyl-2-aryl-3-bromoindole as substrates. The main aim was to study the molecular structure and hydrogen bonding potential of the resultant 3-trifluoroacetyloxime substituted 7-acetamido-2-aryl-3-bromoindole derivatives in the solid state by means of single crystal X-ray diffraction (XRD) technique. The optimized structural parameters (bond lengths, bond angles, and torsion angles) were also investigated by means of density functional theory (DFT) calculations and have been compared with those of the X-ray structure.

## 2. Materials and Methods

### 2.1. General Notes

The melting point values of the prepared compounds were recorded on a Thermocouple digital melting point apparatus and their IR spectra were recorded using a Bruker VERTEX 70 FT-IR Spectrometer (Bruker Optics, Billerica, MA, USA) with a diamond ATR (attenuated total reflectance) accessory by using the thin-film method. Merck kieselgel 60 (0.063–0.200 mm) (Merck KGaA, Frankfurt, Germany) was used as stationary phase for column chromatography. The proton and carbon-13 NMR spectra were obtained as DMSO-$d_6$ solutions using Agilent 300 MHz NMR (Agilent Technologies, Oxford, UK) spectrometer and the chemical shifts are quoted relative to the TMS peak. The low- and high-resolution mass spectra were recorded at an ionization potential of 70 eV using Waters Synapt G2 Quadrupole Time-of-flight mass spectrometer (Waters Corp., Milford, MA, USA). Compounds **1a-d** were prepared as described in our previous investigation [6].

### 2.2. Typical Procedure for the Synthesis of Diketoximes **2a-d**

A stirred mixture of **1a-d** (1 equivalent) and hydroxylamine hydrochloride (2.5 equivalent) in pyridine (30 mL/mmol of **1a-d**) was heated at 80 °C for 12 h. The mixture was cooled to room temperature (RT) and quenched with an ice-cold water and the product was extracted into chloroform. The combined organic layers were washed with water and dried over anhydrous MgSO$_4$. The salt was filtered off and the solvent was evaporated under reduced pressure on a rotary evaporator. The residue was purified by column chromatography on silica gel using 20% EtOAc-hexane mixture as eluent to afford the diketoximes **2a-d**. The following compounds were prepared in this fashion [11].

2.2.1. (*E/Z*)-1-[5-Bromo-7-(1-hydroxyiminoethyl)-2-phenyl-1*H*-indol-3-yl]-2,2,2-trifluoroethanone oxime (**2a**)

A mixture of **1a** (0.50 g, 1.22 mmol), hydroxylamine hydrochloride (0.21 g, 3.05 mmol) in pyridine (40 mL) afforded **2a** (*E* & *Z*-isomers) as a solid (77 g, 0.41%), $R_f$ 0.36; m.p. 223–226 °C; $\nu_{max}$ (ATR) 502, 538, 569, 618, 648, 684, 737, 773, 826, 916, 970, 1011, 1082, 1156, 1206, 1318, 1343, 1398, 1464, 1501, 1531, 1553, 1634, 3243, 3299, 3391, 3446 cm$^{-1}$; $^1$H-NMR (DMSO-$d_6$) 2.31 (H, s, CH$_3$), 7.43–7.62 (7H, m, Ar), 11.14 & 11.20 (1H, s, NH), 11.65 (1H, s, OH), 12.90 and 13.06 (1H, s, OH); $^{13}$C-NMR (DMSO-$d_6$) 11.50, 98.9 & 102.6, 113.4 & 113.6, 118.8 (q, $^1J$ = 280.6 Hz) and 121.6 (q, $^1J$ = 273.7 Hz), 121.7, 122.1 & 122.7, 124.2 & 124.3, 127.3 & 128.2, 129.4 & 129.6, 129.5, 130.8, 131.1 & 131.2, 131.6, 139.0 & 140.2,

140.4 (q, $^2J$ = 31.0 Hz) & 142.0 (q, $^2J$ = 32.1 Hz), 153.7 & 153.8; HRMS (ES): MH$^+$, found: 440.0229. $C_{18}H_{14}N_3O_2F_3{}^{79}Br^+$ requires: 440.0221.

### 2.2.2. (*E/Z*)-1-[5-Bromo-2-(4-fluorophenyl)-7-(1-hydroxyiminoethyl)-1*H*-indol-3-yl]-2,2,2-trifluoroethanone oxime (**2b**)

A mixture of **1b** (0.30 g, 0.65 mmol) and hydroxylamine hydrochloride (0.11 g, 1.45 mmol) in pyridine (40 mL) afforded **2b** as solid (0.21 g, 70%); $R_f$ 0.52; m.p. 288–291 °C; $\nu_{max}$ (ATR) 516, 537, 571, 694, 728, 832, 893, 946, 967, 989, 1011, 1131, 1162, 1184, 1234, 1323, 1373, 1441, 1470, 1506, 1531, 1574, 1652, 3063, 3188, 3411 cm$^{-1}$; $^1$H-NMR (DMSO-$d_6$) 2.15 (3H, s, CH$_3$), 7.13 (1H, d, *J* = 1.8 Hz, H-4), 7.39 (2H, t, *J* = 9.0 Hz, H-3′,5′), 7.57 (2H, t, *J* = 9.0 Hz, H-2′,6′), 7.85 (1H, d, *J* = 1.8 Hz, H-6), 9.78 (1H, s, NH), 11.71 (1H, s, NH), 12.82 (1H, s, OH); $^{13}$C-NMR (DMSO-$d_6$) 24.4, 98.8, 113.0, 116.6 (d, $^2J_{CF}$ = 21.8 Hz), 116.8, 117.0, 121.8 (q, $^1J_{CF}$ = 272.6 Hz), 125.8, 127.0, 128.0 (d, $^4J_{CF}$ = 3.5 Hz), 129.6, 129.7 (d, $^3J_{CF}$ = 8.0 Hz), 137.8, 142.0 (q, $^2J_{CF}$ = 32.2 Hz), 163.0 (d, $^1J_{CF}$ =245.1 Hz), 169.3; HRMS (ES): MH$^+$, found: 458.0130. $C_{18}H_{13}N_3O_2F_4{}^{79}Br^+$ requires: 458.0127.

### 2.2.3. (*E/Z*)-1-[5-Bromo-2-(3-chloro-phenyl)-7-(1-hydroxyiminoethyl)-1*H*-indol-3-yl]-2,2,2-trifluoroethanone oxime (**2c**)

A mixture of **1c** (0.50 g, 1.12 mmol) and hydroxylamine hydrochloride (0.20 g, 2.81 mmol) in pyridine (40 mL) afforded **2c** (*E* & *Z*-isomers) as a solid (0.35 g, 66%), $R_f$ 0.22; m.p. 228–230 °C; $\nu_{max}$ (ATR) 582, 624, 670, 681, 735, 783, 811, 851, 929, 953, 973, 1017, 1077, 1096, 1152, 1178, 1258, 1289, 1319, 1376, 1432, 1462, 1601, 3239, 3284, 3385 cm$^{-1}$; $^1$H-NMR (DMSO-$d_6$) 2.23 (H, s, CH$_3$), 7.38–7.59 (6H, m, Ar), 11.20 and 11.26 (1H, s, NH), 11.55 (1H, s, OH), 12.92 and 13.05 (1H, s, OH); $^{13}$C-NMR (DMSO-$d_6$) 11.60, 98.9 and 103.2, 113.4 and 113.6, 118.6 (q, $^1J$ = 281.7 Hz), 121.7 and 121.9, 123.0, 124.4 and 124.5, 126.0, 127.0, 127.9, 129.2, 130.4, 131.2 and 131.6, 133.1, 134.0, 137.4 and 138.5, 140.0 (q, $^2J$ = 30.8 Hz) and 141.5 (q, $^2J$ = 31.6 Hz), 153.4; HRMS (ES): MH$^+$, found: 473.9833. $C_{18}H_{13}N_3O_2F_3{}^{35}Cl\ ^{79}Br^+$ requires: 473.9832.

### 2.2.4. (*E/Z*)-1-[5-Bromo-7-(1-hydroxyiminoethyl)-2-(4-methoxyphenyl)-1*H*-indol-3-yl]-2,2,2-trifluoroethanone oxime (**2d**)

A mixture of **1d** (0.50 g, 1.14 mmol) and hydroxylamine hydrochloride (0.20 g, 2.84 mmol) in pyridine (40 mL) afforded **2d** (*E* & *Z*-isomers) as a solid (0.35 g, 66%), $R_f$ 0.23; m.p. 211–213 °C; $\nu_{max}$ (ATR) 516, 570, 611, 662, 738, 770, 775, 829, 844, 918, 970, 1032, 1074, 1151, 1175, 1204, 1258, 1287, 1324, 1435, 1466, 1514, 1613, 3237, 3277, 3398 cm$^{-1}$; $^1$H-NMR (DMSO-$d_6$) 2.30 (3H, s, CH$_3$), 3.80 (3H, s, OCH$_3$), 7.09 (2H, d, *J* = 8.7 Hz, H-3′,5′), 7.50–7.53 (4H, m, Ar), 11.00 & 11.04 (1H, s, NH), 11.61 (1H, s, OH), 12.80 and 12.82 (1H, s, OH); $^{13}$C-NMR (DMSO-$d_6$) 11.4, 55.8, 97.9 and 101.7, 113.4 and 114.9, 118.8 (q, $^1J$ = 281.7 Hz), 121.5 and 121.8, 122.4, 123.4 and 123.5, 123.8 and 124.0, 128.7 and 129.5, 130.0, 130.9 and 131.1, 131.4, 139.1 and 140.3, 140.6 (q, $^2J$ = 30.0 Hz) and 142.2 (q, $^2J$ = 32.0 Hz), 153.7 and 153.8, 160.3 and 160.4; HRMS (ES): MH$^+$, found: 470.0331. $C_{19}H_{16}N_3O_3F_3{}^{79}Br^+$ requires: 470.0327.

### *2.3. Typical Procedure for the Beckmann Rearrangement of* **2a**-**d** *into* **3a**-**d**

A stirred mixture of **2** (1 equivalent) and TFA (2 equivalent) in acetonitrile (30 mL/mmol of **2**) was heated at 80 °C for 2 h. The mixture was cooled to RT, quenched with an ice-cold water and the product was extracted with chloroform (3 × 20 mL). The combined organic layers were dried over anhydrous MgSO$_4$ and the salt was filtered off. The solvent was evaporated under reduced pressure and the residue was purified by column chromatography on a silica gel using 60% EtOAc-hexane mixture as an eluent to afford **3** as a solid [11]. The following products were prepared in this fashion:

### 2.3.1. *N*-[5-Bromo-2-phenyl-3-(2,2,2-trifluoro-1-hydroxyiminoethyl)-1*H*-indol-7-yl]acetamide (**3a**)

A mixture of **2a** (0.30 g, 0.68 mmol) and TFA (0.16 g, 1.36 mmol) in acetonitrile (20 mL) afforded **3a** as solid (0.22 g, 73%); $R_f$ 0.50; m.p. 249–252 °C; $\nu_{max}$ (ATR) 531, 585, 603, 691, 728, 764, 844, 892,

908, 1143, 1166, 1199, 1222, 1328, 1368, 1404, 1452, 1468, 1545, 1645, 3058, 3204, 3343 cm$^{-1}$; $^{1}$H-NMR (DMSO-$d_6$) 2.15 (3H, s, CH$_3$), 7.10 (1H, d, *J* = 1.8 Hz, H-4), 7.51–7.55 (5H, m, Ph), 7.86 (1H, d, *J* = 1.8 Hz, 6-H), 9.79 (1H, s, NH), 11.72 (1H, s, NH), 12.80 (1H, s, OH); $^{13}$C-NMR (DMSO-$d_6$) 24.4, 98.8, 113.1, 116.6, 116.9, 121.7 (q, $^{1}J_{CF}$ = 272.6 Hz), 125.9, 126.9, 127.4, 129.5, 129.6, 129.7, 131.4, 138.7, 142.1 (q, $^{2}J_{CF}$ = 33.2 Hz), 169.3; HRMS (ES): MH$^+$, found: 440.0210. C$_{18}$H$_{14}$N$_3$O$_2$F$_3$$^{79}$Br$^+$ requires: 440.0221.

### 2.3.2. *N*-[5-Bromo-2-(4-fluorophenyl)-3-(2,2,2-trifluoro-1-hydroxyiminoethyl)-1*H*-indol-7-yl]acetamide (**3b**)

A mixture of **2b** (0.30 g, 0.65 mmol) and TFA (0.15 g, 1.31 mmol) in acetonitrile (20 mL) afforded **3b** as solid (0.21 g, 70%); $R_f$ 0.52; m.p. 288–291 °C; $\nu_{max}$ (ATR) 516, 537, 571, 694, 728, 832, 893, 946, 967, 989, 1011, 1131, 1162, 1184, 1234, 1323, 1373, 1441, 1470, 1506, 1531, 1574, 1652, 3063, 3188, 3411 cm$^{-1}$; $^{1}$H-NMR (DMSO-$d_6$) 2.15 (3H, s, CH$_3$), 7.13 (1H, d, *J* = 1.8 Hz, H-4), 7.39 (2H, t, *J* = 9.0 Hz, H-3′,5′), 7.55–7.60 (2H, dd, *J* = 5.5 and 8.5 Hz, H-2′,6′), 7.85 (1H, d, *J* = 1.8 Hz, H-6), 9.78 (1H, s, NH), 11.71 (1H, s, NH), 12.82 (1H, s, OH); $^{13}$C-NMR (DMSO-$d_6$) 24.4, 98.8, 113.0, 116.6 (d, $^{2}J_{CF}$ = 21.8 Hz), 116.8, 117.0, 121.8 (q, $^{1}J_{CF}$ = 272.6 Hz), 125.8, 127.0, 128.0 (d, $^{4}J_{CF}$ = 3.5 Hz), 129.6, 129.7 (d, $^{3}J_{CF}$ = 8.0 Hz), 137.8, 142.0 (q, $^{2}J_{CF}$ = 32.2 Hz), 163.0 (d, $^{1}J_{CF}$ =245.1 Hz), 169.3; HRMS (ES): MH$^+$, found: 458.0130 . C$_{18}$H$_{13}$N$_3$O$_2$F$_4$$^{79}$Br$^+$ requires: 458.0127.

### 2.3.3. *N*-[5-Bromo-2-(3-chlorophenyl)-3-(2,2,2-trifluoro-1-hydroxyiminoethyl)-1*H*-indol-7-yl]acetamide (**3c**)

A mixture of **2c** (0.30 g, 0.63 mmol) and TFA (0.14 g, 1.26 mmol) in acetonitrile (20 mL) afforded **3c** as solid (0.21 g, 70%); $R_f$ 0.50; m.p. 280−283 °C; $\nu_{max}$ (ATR) 490, 517, 533, 573, 680, 737, 761, 790, 836, 892, 953, 986, 1061, 1134, 1156, 1189, 1211, 1292, 1322, 1448, 1506, 1544, 1647, 3060, 3219, 3374 cm$^{-1}$; $^{1}$H-NMR (DMSO-$d_6$) 2.16 (3H, s, CH$_3$), 7.15 (1H, d, *J* = 1.8 Hz, H-4), 7.47-7.60 (4H, m, Ar), 7.86 (1H, d, *J* = 1.8 Hz, H-6), 9.78 (1H, s, NH), 11.77 (1H, s, NH), 12.90 (1H, s, OH); $^{13}$C-NMR (DMSO-$d_6$) 24.4, 99.5, 113.2, 117.1, 117.2, 121.7 (q, $^{1}J_{CF}$ = 272.6 Hz), 125.9, 126.1, 126.9, 127.2, 129.3, 129.5, 131.5, 133.4, 134.1, 136.9, 141.8 (q, $^{2}J_{CF}$ = 33.2 Hz), 169.2; HRMS (ES): MH$^+$, found: 473.9829. C$_{18}$H$_{13}$N$_3$O$_2$F$_3$$^{35}$Cl$^{79}$Br$^+$ requires: 473.9832.

### 2.3.4. *N*-[5-Bromo-2-(4-methoxyphenyl)-3-(2,2,2-trifluoro-1-hydroxyiminoethyl)-1*H*-indol-7-yl]acetamide (**3d**)

A mixture of **2d** (0.30 g, 0.64 mmol) and TFA (0.15 g, 1.28 mmol) in acetonitrile (20 mL) afforded **3d** as solid (0.19 g, 65%); $R_f$ 0.37; m.p. 264–266 °C; $\nu_{max}$ (ATR) 524, 577, 594, 736, 755, 831, 892, 948, 966, 985, 1031, 1138, 1174, 1195, 1254, 1306, 1326, 1368, 1401, 1433, 1465, 1505, 1546, 1610, 3004, 3126, 3295 cm$^{-1}$; $^{1}$H-NMR (DMSO-$d_6$) 2.17 (3H, s, CH$_3$), 3.80 (3H, s, CH$_3$), 7.09 (1H, d, *J* = 1.8 Hz, H-4), 7.10 (2H, d, *J* = 8.7 Hz, H-3′,5′),7.50 (2H, d, *J* = 8.7 Hz, H-2′,6′), 7.87 (1H, d, *J* = 1.8 Hz, H-6), 9.79 (1H, s, NH), 11.61 (1H, s, NH), 12.77 (1H, s, OH); $^{13}$C-NMR (DMSO-$d_6$) 24.4, 55.7, 97.9, 114.7 (q, $^{1}J_{CF}$ = 288.5 Hz), 114.9 (2C), 116.7, 123.6, 123.7, 125.7, 126.6, 128.8, 129.8, 138.8, 142.2 (q, $^{2}J_{CF}$ = 32.0 Hz), 160.3, 169.2; HRMS (ES): MH$^+$, found: 470.0331. C$_{19}$H$_{16}$N$_3$O$_3$F$_3$$^{79}$Br$^+$ requires: 470.0327.

### *2.4. Data Collection and Refinement*

Intensity data was determined on a Bruker Venture D8 Photon CMOS diffractometer with graphite-monochromated MoK$\alpha_1$ (λ = 0.71073 Å) radiation at 173 K using an Oxford Cryostream 600 cooler. Data reduction was carried out using the program *SAINT+*, version 6.02 [12] and face-indexed absorption corrections were made using the program *XPREP* [12]. Space group assignment was made using *XPREP* [11]. The structure was solved in the *WinGX* [13] suite of programs by means of direct methods through using *SHELXS-97* [13]. The structure was refined using full-matrix least-squares/difference Fourier techniques on $F^2$ using *SHELXL-2017* [14]. All C–H hydrogen atoms were placed at idealized positions and refined as riding atoms with isotropic parameters 1.2 times those of their parent atoms. All N– and O– bound hydrogen atoms were located in difference map and their coordinates and isotropic displacement parameters refined freely. The disorder of the trifluoroacetyl group was modelled by finding alternate positions for the two CF$_3$ groups in the difference Fourier map. These were then refined anisotropically together with their site occupancies

summed to one to final values of 0.660(19) and 0.340(19). The corresponding C–F bonded distance and the one-angle nonbonded distances were restrained to similar values, subject to s.u. values of 0.01 and 0.02 A, respectively. The disorder of the chloroform solvent sitting on a special position was modelled by finding alternate positions for the H–C–Cl fragments and refining their anisotropic displacement parameters anisotropically and their occupancies to final values of 0.689(14) and 0.311(14). The corresponding C–Cl bonded distance and the one-angle nonbonded distances were restrained to similar values, subject to s.u. values of 0.01 and 0.02 A, respectively. Diagrams and publication material were generated using *ORTEP-3* [13] and *PLATON* [15]. Details of the data collection conditions and the parameters of the refinement process are given in Table 2.

### 2.5. Computational Methods

The density functional theory (DFT) computations were carried out using the B3LYP exchange correlation functional [16], together with 6-311G [17,18] basis set for all atoms. All computations were performed using the Gaussian 09 software suite [19]. The geometrical optimizations were performed in the gas phase without solvent corrections because it was reported that gas phase calculations frequently correspond quite well with crystal structures [20].

## 3. Results and Discussion

### 3.1. Synthesis

The synthetic procedure for the title compounds is shown in Scheme 1. The 7-acetyl-2-aryl-5-bromo-3-(trifluoroacetyl)indoles **1a-d** were subjected to hydroxylamine hydrochloride (2.2 equiv.) in the presence of pyridine in ethanol under reflux for 12 h (Scheme 1). We isolated the corresponding diketoxime derivatives **2a-d** in high yield and purity by aqueous work-up and column chromatography on silica gel (Table 1). Both the $^1$H- and $^{13}$C-NMR spectral data revealed the presence of additional peaks presumably due to different arrangement around the oxime moiety resulting from the known *syn-anti* isomerism [1]. The accurate calculated *m/z* values for these compounds, nevertheless, represent in each case a closet fit consistent with the assigned molecular structures. Whereas the 2-arylindole-3-acetoximes undergo acid-mediated Beckmann rearrangement into 3-acetamido-2-arylindoles with ease [21], the analogous oximes derived from the trifluoroacetyl derivatives are generally stable towards rearrangement into amides [22]. With this literature precedent in mind, we subjected compounds **2a-d** to trifluoroacetic acid-mediated Beckmann rearrangement under reflux for 2 h following the literature precedent [11]. Aqueous work-up and purification of the crude products by silica gel column chromatography afforded compounds characterized by means of NMR, IR, and mass spectrometric methods as the corresponding 3-trifluoroacetyloxime substituted 7-acetamido-2-aryl-5-bromoindole derivatives **3a-d**. The latter are interesting because the α-trifluoromethylated ketoximes can be tosylated or mesylated and then cyclized into the corresponding diaziridines [22–24]. Diaziridines, on the other hand, have been found to readily undergo oxidation into diazirines, which are important in photoaffinity labelling experiments in vivo and in vitro due to their propensity to undergo photochemical reactions to generate carbenes [23,24].
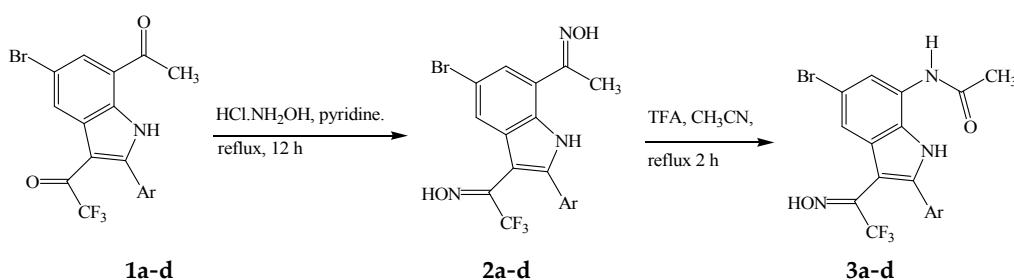


**Scheme 1.** Synthesis of the 7-acetamido-2-aryl-5-bromo-3-(trifluoroacetyloxime)indoles **3a-d**.

**Table 1.** Percentage yields of compounds **2a-d** and **3a-d**.

| Compound | Ar | %Yield of 2 | %Yield 3 |
|:---:|:---:|:---:|:---:|
| a | $C_6H_5-$ | 77 | 73 |
| b | $4-FC_6H_4-$ | 77 | 70 |
| c | $3-ClC_6H_4-$ | 66 | 70 |
| d | $4-MeOC_6H_4-$ | 74 | 65 |

A single crystal of **3d** was obtained by slow evaporation of a chloroform solution, and the molecular structure of compounds **3a-d** was confirmed by X-ray diffraction analysis (CCDC No.: 1822506).

*3.2. X-ray Single Crystal Structure of* **3d**

Chloroform as a solvate has previously been found to play an important role in crystal packing [25] and analysis of the crystal structure of **3d** revealed that it co-exists with a chloroform solvate in the ratio 3:1 (Figure 1). There is evidence of existence of halogen bonding between chloroform molecule and **3d**. The 2-aryl ring of **3d** is twisted out of plane of co-planarity to avoid steric interaction with the trifluoroacetyl oxime moiety with torsion angles C(9)–C(8)–C(10)–C(11) and N(1)–C(8)–C(10)–C(15) of −140.0° and −144.2°, respectively. There is intramolecular hydrogen bonding between the amide oxygen and hydrogen atom attached to the indole nitrogen (N–1; Figure 2) with N(1)–H(1)···O(3) bond distance of 2.00 Å and bond angle ∠(DHA) = 135° (Table 2). The molecules are also bound together by several intermolecular hydrogen bonds (Figure 2). There is evidence of indole stacking in the crystal structure of **3d** with distances of 3.4 Å and 4.0 Å between the planes and the centroids, respectively (Figure 3). However, π-stacking has not been observed before in the crystal structure of the analogous 5-methoxy-1-methylindole-3-carboxaldehyde oxime derivative [26]. The crystal structure of **3d** also revealed the presence of the aromatic CH–π interactions with distances C···centroid = 2.6 Å and angle CH···centroid = 158° (Figure 4). CH–π hydrogen bond has been found to play significant role in crystal packing, the structure of clathrates, solid-state reactions, and drug design [27]. Strong intermolecular hydrogen bonding exists between the amide oxygen of one molecule and the hydroxyl proton of the other with O(2)–H(2)···O(3) bond distance and bond angle of 1.64 Å and 170°, respectively. Intermolecular hydrogen bonding also exists between the amide proton of one molecule and oxygen atom of the oxime moiety of another molecule with bond distance and bond angle of N(3)–H(3)···O(2) = 2.17 Å and 177°, respectively. The structure also presents 6-membered rings formed through halogen bonds (C–Br···Br) with Br···Br distances of 3.7 Å (Figure 5). Some examples of similar situations in which bromine plays an important role in crystal packing have been described in the literature [28,29]. Crystal data and structure refinement for compound **3d** are represented in Table 3.



(**a**) XRD　　　　　　　　　　　　　　　　　(**b**) Computed
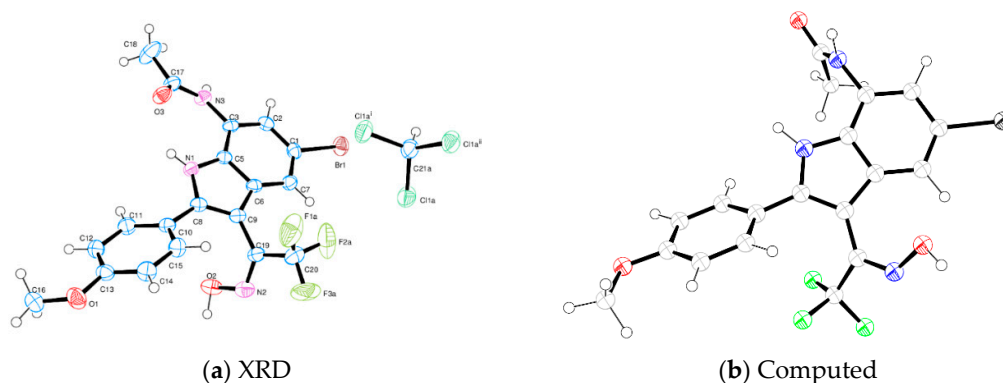
**Figure 1.** (**a**) The Oak Ridge Thermal Ellipsoid Plot (ORTEP) diagram of **3d** showing crystallographic labelling. Displacement ellipsoids are drawn at the 50% probability level; (**b**) A view of the optimized structure of **3d** from density functional theory (DFT) calculations.
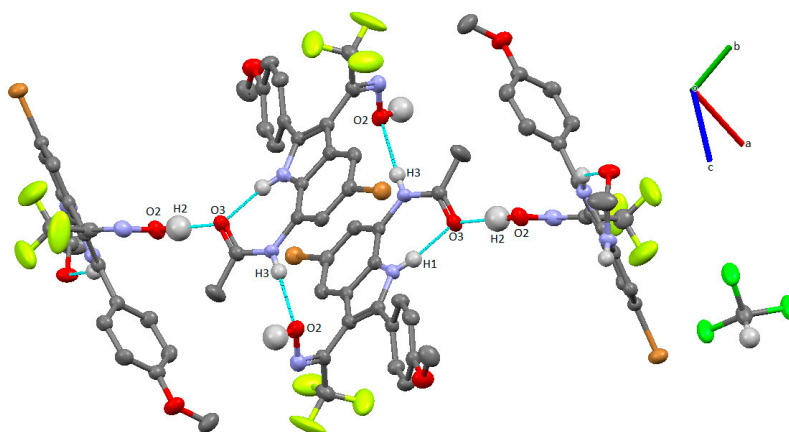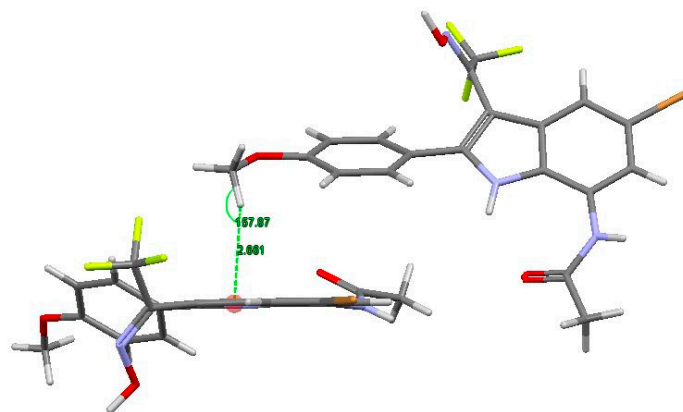
**Figure 2.** Compound **3d** showing intra- and intermolecular hydrogen bonding.

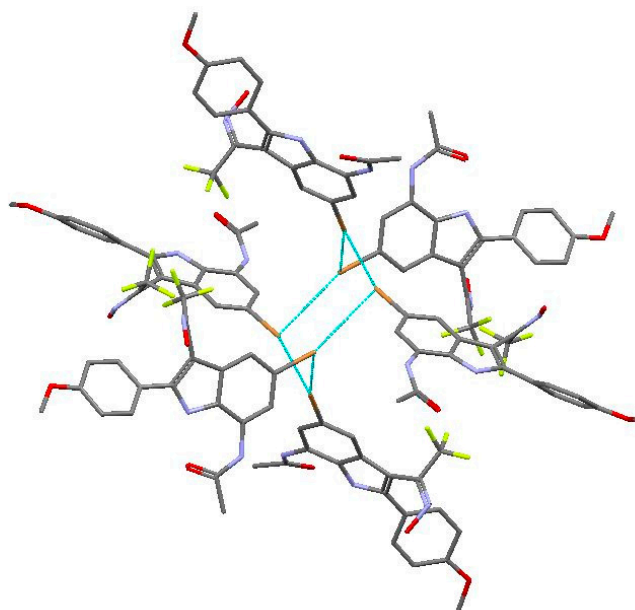**Table 2.** Selected hydrogen bonding interactions in compound **3d**.

| D–H⋯A | d(D–H)d | d(H⋯A) | d(D⋯A) | ∠(DHA) |
|---|---|---|---|---|
| N(1)–H(1)⋯O(3) | 0.85(3) | 2.00(2) | 2.668(2) | 135(2) |
| N(3)–H(3)⋯O(2)#3 | 0.80(3) | 2.17(3) | 2.968(2) | 177(2) |
| O(2)–H(2)⋯O(3)#4 | 0.96(4) | 1.64(4) | 2.597(2) | 170(3) |
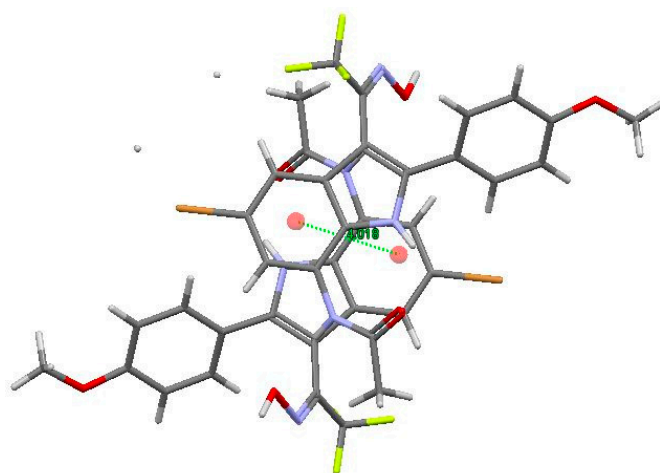


**Figure 3.** Indole stacking in the crystal structure of **3d**.



**Figure 4.** Structure of **3d** showing CH–π bond interaction.

**Figure 5.** 6-membered rings formed through halogen bonds (C–Br···Br) between molecules of **3d**.

**Table 3.** Crystal data and structure refinement for compound **3d**.

| CCDC No.: 1822506 | | | |
|---|---|---|---|
| Formula | $C_{19}H_{15}BrClF_3N_3O_3$ | Refinement method | Full-matrix least-squares on $F^2$ |
| Formula weight | 469.02 | Data/restraints/parameters | 3916/58/329 |
| Temperature | 173(2) K | Measured reflections | 122613 |
| Wavelength | 0.71073 Å | $\theta_{min}/\theta_{max}$ | 2.804/25.499° |
| Crystal system | Trigonal | $R_{int}$ | 0.0588 |
| Space group | R-3:H | Goodness-of-fit on $F^2$ | 1.027 |
| Unit cell dimensions | a = 25.1614(13) Å<br>b = 25.1614(13) Å<br>c = 17.3032(9) Å<br>$\alpha = 90°$<br>$\beta = 90°$.<br>$\gamma = 120°$ | Final $R$ indices<br>[I > 2σ (I)] | $R_1$ = 0.0282<br>$wR_2$ = 0.0681 |
| Volume | 9486.9(11) Å$^3$ | $R$ indices (all data) | $R_1$ = 0.0366<br>$wR_2$ = 0.0729 |
| Z | 6 | Largest diff. peak/hole | 0.359/−0.367 e.Å$^{-3}$ |
| Density (calcd.) | 1.607 Mg/m$^3$ | | |
| Absorption coefficient | 2.129 mm$^{-1}$ | | |
| F(000) | 4596 | | |
| Crystal size | 0.384 × 0.063 × 0.062 mm$^3$ | | |

## 3.3. Optimized Geometry of **3d**

The optimized structure of **3d** is shown in Figure 1b above and was obtained by the density functional theory (DFT) method using hybrid functional Becke's three parameter nonlocal exchange functional with the Lee-Yang-Parr correlation function (B3LYP) and the 6-311G basis set. Some of the optimized parameters, namely, the bond lengths, bond angles, and torsion angles are given in Table 4 and they have been assigned in accordance with the XRD atomic numbering scheme given in Figure 1a. The conformation of the 2-arylindole framework of the optimized structure of **3d** in the gas phase resembles that of the XRD structure with a slight difference on the orientation of the acetamido and 3-trifluoroacetyloxime groups. These deviations are presumably due to the involvement of these groups in intermolecular interactions in the solid state (see Figure 2) in which case the molecules are linked by

the crystal field along intermolecular interactions. There are no significant differences between the experimentally determined structural parameters and those predicted using the DFT method.

**Table 4.** Selected experimental and theoretical bond lengths (Å) and angles (°) of **3d.**

| Geometric Parameters | X-ray | DFT |
|---|---|---|
| **Bond lengths (Å)** | | |
| C(3)–N(3) | 1.416(3) | 1.433 |
| C(8)–N(1) | 1.377(3) | 1.388 |
| C(8)–C(10) | 1.462(3) | 1.466 |
| C(9)–C(19) | 1.472(3) | 1.448 |
| C(13)–O(1) | 1.361(3) | 1.405 |
| C(16)–O(1) | 1.413(3) | 1.455 |
| C(17)–O(3) | 1.236(3) | 1.012 |
| C(17)–N(3) | 1.335(3) | 1.390 |
| C(19)–N(2) | 1.277(3) | 1.331 |
| C(19)–C(20) | 1.502(3) | 1.495 |
| **Bond angles (°)** | | |
| C(5)–N(1)–C(8) | 110.2(18) | 110.4 |
| C(15)–C(10)–C(8) | 120.6(19) | 120.4 |
| N(3)–C(17)–C(18) | 116.5(2) | 116.9 |
| N(2)–C(19)–C(9) | 126.9(2) | 127.0 |
| C(17)–N(3)–C(3) | 129.8(19) | 126.8 |
| **Torsion angles (°)** | | |
| N(1)–C(8)–C(10)–C(15) | −144.2(2) | −145.0 |
| O(3)–C(17)–N(3)–C(3) | −2.6(4) | −1.3 |
| C(14)–C(13)–O(1)–C(16) | −177.8(2) | −177.4 |

The HOMO (highest occupied molecular orbital) and LUMO (lowest unoccupied molecular orbital) are important factors mostly used as descriptors in Quantitative Structure Activity Relationship (QSAR) [30]. The HOMO and LUMO surfaces of compound **3d** were computed at the B3LYP/6-311G level and these are represented in Figure 6. DFT calculations revealed that the HOMO is mainly localized on the 2-arylindole framework and the α-trifluoromethylated ketoxime function and partially on oxygen atom of the methoxy group. The LUMO, on the other hand, is localized mainly on the aromatic framework and partially on the α-trifluoromethylated ketoxime, methoxy, and the amide functions. The value of the energy separation between HOMO and LUMO is −0.10476 eV and this small energy gap could indicate that the title structure can be excited using minimal energy.



HOMO (−0.28560 eV)          LUMO (−0.18084 eV)
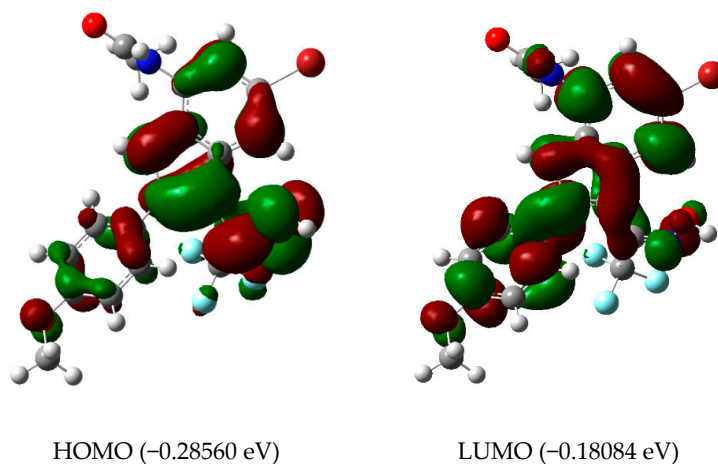
**Figure 6.** Frontier molecular orbitals of **3d** using the B3LYP/6-311++G(d,p) basis set.

## 4. Conclusions

The diketoximes **2a-d** and the 7-acetamido-2-aryl-3-(trifluoroacetyloxime)indoles **3a-d**, were synthesized and characterized using a combination of spectroscopic techniques. The three-dimensional structure of compounds **3a-d** was further confirmed using single crystal X-ray diffraction on a representative compound **3d**. The crystal structure revealed the presence of strong intramolecular and intermolecular hydrogen bonds as well as aromatic CH–π and C–Br···Br, which play significant role in the crystal packing. The X-ray structure and the DFT optimized counterpart calculated by the B3LYP/6-311G basis set compare favourably and the optimized geometry reproduced the crystal structure parameters well. Since a strong hydrogen bond acceptor (e.g., acetyl, formyl or trifluoroacetyl group) at the C-3 position of the indole framework enhances anticancer activity [5,6], the presence of a dual hydrogen bond donating and accepting ketoxime moiety in this position makes compounds **3** suitable candidates for evaluation of biological activity as potential anticancer agents to correlate between structural variation and cytotoxicity. Molecular docking (in silico) could be used to predict the hypothetical protein-ligand binding mode against tubulin or other relevant examples of enzyme kinases to guide further structure activity relationship (SAR). The α-trifluoromethylated ketoxime moiety also represents suitable template for further transformation into the corresponding α-trifluoromethylated amines or diazirines.

**Conflicts of Interest:** There is no conflict of interest.

## References

1. Abele, E.; Abele, R.; Dzenitis, O.; Lukevics, E. Indole and isatin oximes: Synthesis, reactions, and biological activity. *Chem. Heterocycl. Compd.* **2003**, *39*, 3–35. [CrossRef]
2. Bertolasi, V.; Gilli, G.; Veronese, A. Structures of *E,E*-3-(*p*-tolylimino)-2-butanone oxime and *E,Z*-4-(*p*-tolylimino)-2,3-pentanedione 3-oxime. An X-ray crystallographic investigation on bonding in oximes. *Acta Crystallogr. Sect. B* **1982**, *B38*, 502–511. [CrossRef]
3. Desiraju, G.; Steiner, T. *The Weak Hydrogen Bond–in Structural Chemistry and Biology*; Oxford University Press: New York, NY, USA, 1999.
4. Hadzi, D.; Kidric, J.; Koller, J.; Mavrij, J. The role of hydrogen bonding in drug-receptor interactions. *J. Mol. Struct.* **1990**, *237*, 139–150. [CrossRef]
5. Watterson, S.H.; Dhar, T.G.M.; Ballentine, S.K.; Shen, Z.; Barrish, J.C.; Cheney, D.; Fleener, C.A.; Roleau, K.A.; Watterson, R.T.S.H.; Dhar, T.G.M.; et al. Novel indole-based inhibitors of IMPDH: Introduction of hydrogen bond acceptors at indole C-3. *Bioorg. Med. Chem. Lett.* **2003**, *13*, 1273–1276. [CrossRef]
6. Mphahlele, M.J.; Pabhoo, N. Synthesis, evaluation of cytotoxicity and molecular docking studies of the 7-acetamido substituted 2-aryl-5-bromo-3-trifluoroacetylindoles as potential inhibitors of tubulin polymerization. *Pharmaceuticals* **2018**, *11*, 59. [CrossRef] [PubMed]
7. Kool, E.T. Hydrogen bonding, base stacking, and steric effects in DNA replication. *Annu. Rev. Biophys. Biomol. Struct.* **2001**, *30*, 1–22. [CrossRef] [PubMed]
8. Mishra, S.K.; Suryaprakash, N. NMR research centre, solid state and structural chemistry, intramolecular hydrogen bonding involving organic fluorine: NMR investigations corroborated by DFT-based theoretical calculations. *Molecules* **2017**, *22*, 423. [CrossRef] [PubMed]
9. Cheng, G.; Wu, Q.; Shang, Z.; Liang, X.; Lin, X. Stereoselective transformations of α-trifluoromethylated ketoximes to optically active amines by enzyme-nanometal cocatalysis: Synthesis of (*S*)-inhibitor of phenylethanolamine *N*-methyltransferase. *ChemCatChem* **2014**, *6*, 2129–2133. [CrossRef]

10. Hu, H.; Wu, J.; Ao, M.; Wang, H.; Zhou, T.; Xue, Y.; Qiu, Y.; Fang, M.; Wu, Z. Synthesis, structure–activity relationship studies and biological evaluation of novel 2,5-disubstituted indole derivatives as anticancer agents. *Chem. Biol. Drugs Des.* **2016**, *88*, 766–778. [CrossRef] [PubMed]

11. Mphahlele, M.J.; Mmmonwa, M.M.; Choong, S.Y. Synthesis and evaluation of *N*-(3-trifluoroacetylindol-7-yl) acetamides for potential in vitro antiplasmodial properties. *Molecules* **2017**, *22*, 1099. [CrossRef] [PubMed]

12. *Bruker, APEX-3, SAINT+*; Version 6.02 (Includes XPREP and SADABS); Bruker AXS Inc.: Madison, WI, USA, 2016.

13. Sheldrick, G.M. A short history of SHELX. *Acta Cryst. C* **2015**, *71*, 3–8. [CrossRef] [PubMed]

14. Farrugia, L.J. ORTEP-3 for Windows-a version of ORTEP-III with a Graphical User Interface (GUI). *J. Appl. Crystallogr.* **2012**, *45*, 849–854. [CrossRef]

15. Spek, A.L. Structure validation in chemical crystallography. *Acta Cryst. D* **2009**, *65*, 148–155. [CrossRef] [PubMed]

16. Becke, A.D. Density-functional thermochemistry III. The role of exact exchange. *J. Chem. Phys.* **1993**, *98*, 5648–5652.

17. Lee, C.; Yang, W.; Parr, R.G. Development of the Colle-Salvetti correlation-energy formula into a functional of the electron density. *Phys. Rev. B* **1988**, *37*, 785–789. [CrossRef]

18. Krishnan, R.; Binkley, J.S.; Seeger, R.; Pople, J.A. Self-consistent molecular orbital methods. XX. A basis set for correlated wave functions. *J. Chem. Phys.* **1980**, *72*, 650–654.

19. Frisch, M.J.; Trucks, G.W.; Schlegel, H.B.; Scuseria, G.E.; Robb, M.A.; Cheeseman, J.R.; Scalmani, G.; Barone, V.; Mennucci, B.; Petersson, G.A.; et al. *Gaussian 09, Revision A.01*; Gaussian Inc.: Wallingford, CT, USA, 2009.

20. Honarparvar, B.; Govender, T.; Maguire, G.E.; Soliman, M.E.; Kruger, H.G. Integrated approach to structure-based enzymatic drug design: Molecular modeling, spectroscopy, and experimental bioactivity. *Chem. Rev.* **2013**, *114*, 493–537. [CrossRef] [PubMed]

21. Qu, J.; Kumar, N.; Alamgir, M.; Balck, D.S. A versatile synthetic route to 11*H*-indolo[3,2-*c*]isoquinolines. *Tetrahedron Lett.* **2009**, *50*, 5628–5630. [CrossRef]

22. Strømgaard, K.; Saito, D.R.; Shindou, H.; Ishii, S.; Shimizu, T.; Nakanishi, K. Ginkgolide derivatives for photolabeling studies: Preparation and pharmacological evaluation. *J. Med. Chem.* **2002**, *45*, 4038–4046. [CrossRef] [PubMed]

23. Wartmann, T.; Lindel, T. *L*-Phototryptophan. *Eur. J. Org. Chem.* **2013**, *2013*, 1649–1652. [CrossRef]

24. Protasova, I.; Bulat, B.; Jung, N.; Bräse, S. Synthesis of diaziridines and diazirines via resin-bound sulfonyl oximes. *Org. Lett.* **2017**, *19*, 34–37. [CrossRef] [PubMed]

25. Allen, F.H.; Wood, P.A.; Galek, P.T.A. Role of chloroform and dichloromethane solvent molecules in crystal packing: An interaction propensity study. *Acta Cryst.* **2013**, *B69*, 379–388. [CrossRef] [PubMed]

26. Janes, R.W.; Potter, B.S.; Naylor, M.A.; Ferguson, A.C.; Patel, K.B.; Stratford, M.R.L.; Wardman, P.; Evertt, S.A. 1-Methylindole-3-carboxaldehyde oxime derivatives. *Acta Cryst.* **2001**, *C57*, 58–61. [CrossRef]

27. Nishio, M. CH/π hydrogen bonds in crystals. *CrystEngComm* **2004**, *6*, 130–158. [CrossRef]

28. Aakerōy, C.B.; Fasulo, M.; Schultheiss, N.; Desper, J.; Moore, C. Structural competition between hydrogen and halogen bonds. *J. Am. Chem. Soc.* **2007**, *129*, 13772–13773. [CrossRef] [PubMed]

29. Tero, T.-R.; Salorinne, K. The effect of halogen bonding on the packing of bromine-substituted pyridine and benzyl functionalized resorcinarene tetrapodants in the solid state. *CrystEngComm* **2012**, *14*, 7360–7367. [CrossRef]

30. Clare, B.W. Frontier orbital energies in quantitative structure-activity relationships: A comparison of quantum chemical methods. *Theor. Chim. Acta* **1994**, *87*, 415–430. [CrossRef]